



# Molecular dynamics investigation of MgO–CaO–SiO<sub>2</sub> liquids: Influence of pressure and composition on density and transport properties

Liqun Zhang, James A. Van Orman\*, Daniel J. Lacks

Department of Geological Sciences, Case Western Reserve University, Cleveland, OH 44106, United States

Department of Chemical Engineering, Case Western Reserve University, Cleveland, OH 44106, United States

## ARTICLE INFO

### Article history:

Received 19 February 2010

Received in revised form 20 April 2010

Accepted 23 April 2010

Editor: D.B. Dingwell

### Keywords:

Silicate melt  
Transport properties  
Diffusion  
Viscosity  
Magma  
Differentiation

## ABSTRACT

Molecular dynamics simulations are carried out to address the influence of pressure and composition on the properties of liquids in the MgO–CaO–SiO<sub>2</sub> system. At low pressure the mixing of liquids with different SiO<sub>2</sub> fractions is highly non-ideal, while mixing of liquids with the same SiO<sub>2</sub> fraction is nearly ideal; at high pressure, mixing becomes ideal for all systems. At low pressure, the viscosity and diffusivity of network forming ions, and their activation volumes, can change dramatically with changes in the SiO<sub>2</sub> fraction of the liquid; at high pressure, the dependence of these properties on composition is relatively small, and the Ca/Mg ratio has an influence comparable to the SiO<sub>2</sub> fraction. In general, the properties of the MgO–CaO–SiO<sub>2</sub> system become much simpler at high pressure – in contrast to the situation at low pressure, at high pressure mixing is ideal, the transport properties are relatively insensitive to composition, and there are no anomalous property changes with pressure.

© 2010 Elsevier B.V. All rights reserved.

## 1. Introduction

Molecular simulation is an increasingly important tool to gain insight into the structural, transport and thermodynamic properties of silicate liquids. Simulations are particularly important for investigating silicate liquid properties under conditions that are difficult to access experimentally, for example at the very high pressures and temperatures that are relevant to the early large-scale differentiation of the Earth. Most molecular simulation studies of molten oxides and silicates have focused on one-component (e.g. Alfè, 2005; Stixrude and Karki, 2005; Karki et al., 2006, 2007; Adjaoud et al., 2008; de Koker et al., 2008; Ben Martin et al., 2009; Nevins et al., 2009) and two-component (Kubicki et al., 1990; Bryce et al., 1999; Lacks and Van Orman, 2007) systems. Here we present a molecular dynamics study of liquids in the ternary CaO–MgO–SiO<sub>2</sub> system, which encompasses three of the geologically most abundant oxide components. The density, excess molar volume, and transport properties of the liquids, and their variation with chemical composition and pressure, are presented. To elucidate the mixing properties, several binary joins (CaO–SiO<sub>2</sub>, MgO–SiO<sub>2</sub>, CaO–MgO and CaSiO<sub>3</sub>–MgSiO<sub>3</sub>) are investigated in detail.

The physical basis for the properties are interpreted in terms of the atomic level structure of the liquid, which can be considered as a

framework of linked SiO<sub>4</sub> tetrahedra together with non-framework species such as Mg and Ca (e.g., Mysen, 1988). If the linked SiO<sub>4</sub> tetrahedra percolate throughout the system, the structure is said to be “polymerized”. Non-framework species disrupt the polymerization, and so the extent of polymerization is greatest in silica-rich liquids. It is well known that the extent of polymerization plays a dominant role in the transport properties of silicate liquids, as the percolated linkages act to ‘lock’ the system in place. Thus more highly polymerized structures have larger viscosities, and changes in composition that alter the extent of polymerization can change the viscosity by many orders of magnitude (e.g., Giordano and Dingwell, 2003). The extent of polymerization also determines the pressure dependence of viscosities: viscosities of less polymerized liquids increase with pressure, as expected from free volume arguments, while viscosities of highly polymerized liquids anomalously decrease with pressure (Scarfè et al., 1987; Suzuki et al., 2002; Behrens and Schulze, 2003; Reid et al., 2003; Tinker et al., 2004; Liebske et al., 2005). The anomalous decrease in viscosity with increasing pressure occurs because the open tetrahedral framework structure of SiO<sub>2</sub> collapses under high pressure, thereby destroying the polymerization that leads to high viscosity. While the above discussion focused on viscosity, analogous changes occur for the diffusivity of framework species (Si and O), with the changes in diffusivity being opposite in direction to those of viscosity (Mikkelsen, 1984; Shimizu and Kushiro, 1984; Lesher et al., 1996; Poe et al., 1997; Reid et al., 2001; Tinker and Lesher, 2001; Tinker et al., 2003).

\* Corresponding author. Department of Chemical Engineering, Case Western Reserve University, Cleveland, OH 44106, United States. Tel.: +1 216 368 3765; fax: +1 216 368 3691. E-mail address: [james.vanorman@case.edu](mailto:james.vanorman@case.edu) (J.A. Van Orman).

## 2. Simulation methods

The simulations are carried out for the compositions shown in Fig. 1, and at pressures ranging from 0 to 20 GPa. All simulations are carried out at 3000 K, which is the lowest temperature for which we can obtain equilibrated results for all compositions within a ~30 ns simulation (note that the silica-rich systems at low pressure are the slowest to equilibrate). The simulations are carried out with the LAMMPS software package, version 2001 (Plimpton, 1995; <http://lammmps.sandia.gov>).

A modified version of the BKS force field (van Beest et al., 1990) is used for the atomic interactions. The non-Coulombic potential between atoms  $i$  and  $j$ ,  $U_{ij}(r)$ , is of the form

$$U_{ij}(r) = \phi_{ij}(r) - \phi_{ij}(r_c), \quad r \leq r_c \quad (1a)$$

$$U_{ij}(r) = 0, \quad r > r_c \quad (1b)$$

$$\phi_{ij}(r) = A_{ij} \exp(-B_{ij}r_j) - C_{ij}/r^6 + \varepsilon_{ij}[(\sigma_{ij}/r)^{30} - (\sigma_{ij}/r)^6]. \quad (1c)$$

The parameters for the force field are given in Table 1; the  $A$ ,  $B$  and  $C$  parameters for Si–O and O–O interactions are from van Beest et al. (1990), and the parameters for Mg–O and Ca–O interactions are obtained by fitting to experimental pressure–volume data for crystalline MgO (Speziale et al., 2001) and CaO (Speziale et al., 2006). Following van Beest et al. (1990), the non-Coulombic interactions for cation–cation pairs are zero. The non-Coulombic potential is cutoff at  $r_c = 5.5$  Å. The final term in Eq. (1c) is not from the BKS force field, but is a very short ranged repulsive interaction that prevents non-physical behavior as the atoms approach each other very closely. Coulombic interactions are calculated using the Particle-Mesh Ewald method (Plimpton et al., 1997), with a cutoff distance of 10 Å and an accuracy criterion of  $10^{-4}$  Å.

For each system, we determine the equilibrium volume using molecular dynamics simulation in the NPT ensemble, where the number of particles ( $N$ ), the pressure ( $P$ ), and the temperature ( $T$ ) are fixed. The temperature and pressure control are achieved with the Nosé-Hoover thermostat and barostat, respectively. The NPT simulation is run for at least 4 ns, at the end of which the system volume fluctuates consistently about the equilibrium volume. Next, the viscosity and diffusivity are determined using molecular dynamics simulation in the NVT ensemble, where the system volume ( $V$ ) is fixed, instead of pressure, at the equilibrium volume previously determined in the NPT simulation. The NVT simulations are carried out for 5 to 30 ns (longer simulation times are used for more slowly relaxing systems). A time step of 1 fs is used in all simulations, and the atom positions are output every 1 ps. Approximately 2000 atoms are

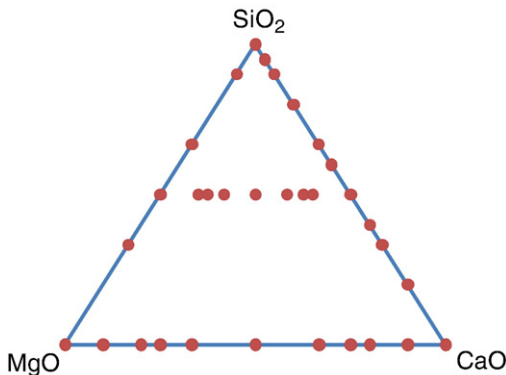


Fig. 1. Compositions of the MgO–CaO–SiO<sub>2</sub> system examined in the simulations.

Table 1

Potential parameters for non-Coulombic interactions.

	$A$ (kJ/mol)	$B$ (Å <sup>-1</sup> )	$C$ (kJ/mol Å <sup>6</sup> )	$\varepsilon$ (kJ/mol)	$\sigma$ (Å)
O–O	133,996	2.7600	16,884.9	0.4056	1.7792
Si–O	1,737,095	4.8732	12,884.4	1.1956	1.3136
Mg–O	315,000	3.79749	9648.5	1.1956	1.7
Ca–O	600,740	3.75892	13,265.2	1.1956	1.7

included in each simulation (the specific number varies with the composition of the system). To remove surface effects, periodic boundary conditions are used.

The equilibrium molar volumes are obtained from the NPT simulations. The excess molar volumes,  $V_E$ , which represent the deviations between the real molar volumes and the values based on ideal binary mixing, are calculated as

$$V_E = V - x_A V_A - x_B V_B \quad (2)$$

Here,  $V_A$  and  $V_B$  are the molar volume of pure component  $A$  and pure component  $B$ , respectively.

The viscosities and diffusivities are obtained from the results of the NVT simulations. The Green-Kubo formula is used to calculate the viscosity,  $\eta$ , by integrating the off-diagonal component of the stress-tensor,

$$\eta = \frac{V}{kT} \int_0^\infty \langle \sigma_{xy}(t) \sigma_{xy}(0) \rangle dt \quad (3)$$

where  $k$  is Boltzmann's constant, and  $\sigma_{xy}(t)$  is the off-diagonal component of the stress tensor in the  $xy$  direction at time  $t$ , and  $\langle \rangle$  denotes an ensemble average. The uncertainty in each calculation of viscosity is estimated from the difference in the results obtained using  $\sigma_{xy}$ ,  $\sigma_{yz}$  and  $\sigma_{zx}$ . The diffusion coefficient of atom type  $i$ ,  $D_i$ , is calculated using the Einstein method,

$$D_i = \frac{\langle (x_i(t) - x_i(0))^2 \rangle}{2t} \quad t \rightarrow \infty. \quad (4)$$

Here,  $x_i(t)$  is the  $x$ -coordinate of an atom of type  $i$  at time  $t$ . We averaged the diffusion coefficient results for each atom of the same type, and the uncertainty estimate is obtained from the difference in the results in the  $x$ ,  $y$ , and  $z$  directions. To reduce the noise in  $\sigma_{ij}(t)$  and  $x_i(t)$ , the results are averaged over many initial times – i.e., the mean squared displacement at 10 ps is the average of contributions from  $x_i$  (10 ps) to  $x_i$  (0 ps),  $x_i$  (11 ps) to  $x_i$  (1 ps),  $x_i$  (12 ps) to  $x_i$  (2 ps), etc. Thus, longer simulation times decrease the noise in these properties, as there are more contributions used to obtain the averages.

Data used to determine the viscosity and diffusivity, for SiO<sub>2</sub> at  $P=0$ , are shown in Fig. 2. These results show that this liquid fully relaxes and equilibrates on the timescale of 1 ns – i.e., at this timescale, the stress autocorrelation function (the integrand of Eq. (3)) decays to 0, and the mean-squared displacement displays true diffusive behavior (power law with exponent of 1). Of all systems examined here, the relaxations are slowest for SiO<sub>2</sub> at  $P=0$ ; thus, the results of Fig. 2 demonstrate that all results presented here represent results for ergodic and equilibrated systems (since all relaxation times are less than ~1 ns, and the simulation times are 5–30 ns).

The dependence of the diffusion coefficients and viscosity on pressure is often represented in terms of Arrhenius equations,

$$D_i = D_{i,0} \exp\left(\frac{-(E_i + PV_i)}{kT}\right) \quad (5)$$

$$\frac{1}{\eta} = \frac{1}{\eta_0} \exp\left(\frac{-E_\eta + PV_\eta}{kT}\right) \quad (6)$$

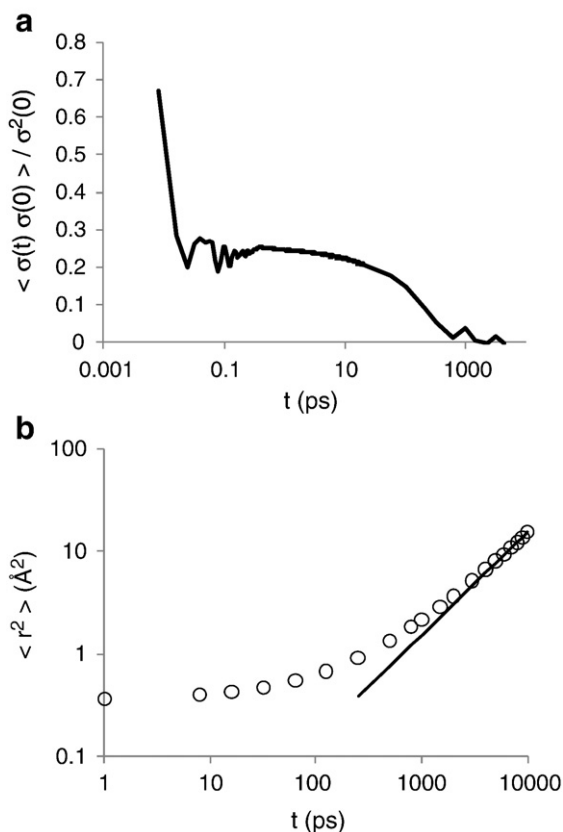


**Fig. 2.** Intermediate quantities used to determine transport properties, for SiO<sub>2</sub> at  $P=0$ . (a) Normalized stress auto-correlation function (integrand of Eq. (3)) as a function of time. (b) Mean squared displacement as a function of time; the line shows a power law with exponent 1.

where  $V$  is the apparent activation volume and  $E$  is the activation energy for the property of interest, and  $D_{i,0}$  and  $\eta_0$  are the diffusion coefficient and viscosity extrapolated to infinite temperature. In general,  $E$  and  $V$  are not constants, but can depend on temperature and pressure – in fact, for some systems the value of  $V$  changes sign with changing pressure. Thus  $V$  does not always have clear physical significance, and for this reason we refer to it as the ‘apparent’ activation volume.

### 3. Results

Simulations are carried out along four joins: (1) MgO–SiO<sub>2</sub>; (2) CaO–SiO<sub>2</sub>; (3) MgSiO<sub>3</sub>–CaSiO<sub>3</sub>; and (4) MgO–CaO, at temperature  $T=3000$  K and pressures between 0 and 20 GPa.

#### 3.1. Molar volumes

The results for the molar volumes are given in Table 2 and Fig. 3; Table 2 gives the molar volumes for the end-members of the joins, and Fig. 3 gives the deviations of the molar volumes of the mixtures from

**Table 2**  
Molar volume results (cm<sup>3</sup>/mol), at  $T=3000$  K.

	$V$ ( $P=0$ )	$V$ ( $P=20$ GPa)
SiO <sub>2</sub>	26.75	16.41
MgO	16.34	11.73
CaO	24.40	15.93
MgSiO <sub>3</sub>	41.48	27.77
CaSiO <sub>3</sub>	50.17	32.24

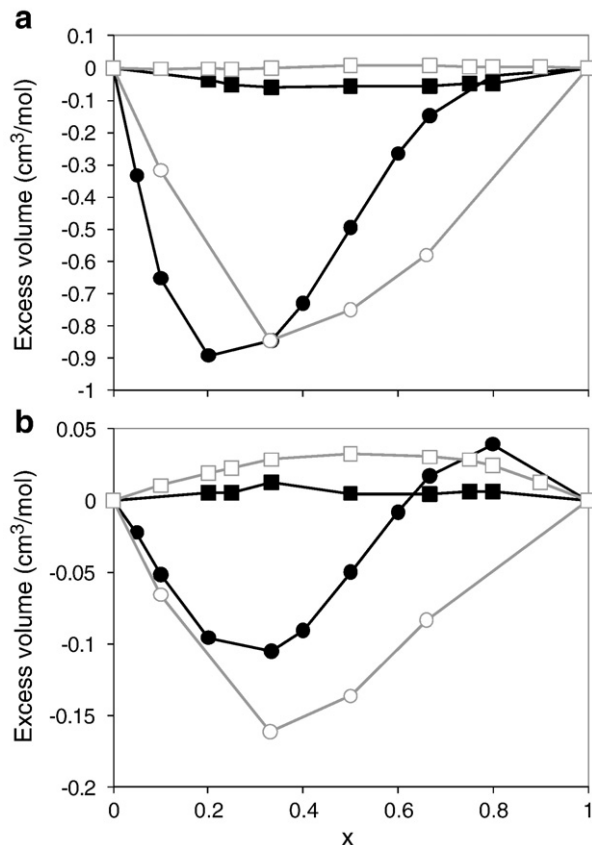


**Fig. 3.** Excess volume of mixing, along four joins. Open circles: MgO–SiO<sub>2</sub>; Filled circles: CaO–SiO<sub>2</sub>; Open squares: CaO–MgO; Filled squares: CaSiO<sub>3</sub>–MgSiO<sub>3</sub>. (a)  $P=0$  GPa; and (b)  $P=20$  GPa.

ideal mixing of the end-members (i.e. the excess molar volumes). The following conclusions are evident from Fig. 3: (1) mixing is nearly ideal when the fraction of SiO<sub>2</sub> does not change; and (2) mixing becomes nearly ideal for all systems at higher pressures (e.g., 20 GPa). The physical basis for these changes in the ideality of mixing are addressed in the Discussion section below.

#### 3.2. Transport properties: Effect of SiO<sub>2</sub> fraction

Fig. 4 shows all simulation results for the viscosity and O diffusivity, plotted as a function of SiO<sub>2</sub> fraction – note that in many cases more than one result is shown at a given value of SiO<sub>2</sub> fraction (e.g., all results along the MgSiO<sub>3</sub>–CaSiO<sub>3</sub> join have the same SiO<sub>2</sub> fraction). It is clear from this figure that, at low pressure, SiO<sub>2</sub> fraction is the primary factor that controls the viscosity and diffusivity in these systems. At  $P=0$ , the viscosity and oxygen diffusivity change by almost 3 orders of magnitude as the SiO<sub>2</sub> fraction changes; in contrast, variation in the Mg/Ca ratio has only a small effect at  $P=0$ . However, at  $P=20$  GPa the dependence on SiO<sub>2</sub> fraction and Mg/Ca ratio become comparable: the effect of SiO<sub>2</sub> fraction is weakened (less than 1 order of magnitude change as the SiO<sub>2</sub> fraction changes), while the effect of Mg/Ca ratio is strengthened. The influence of the Mg/Ca ratio is addressed in more detail below.

It is also evident in Fig. 4 that the viscosity increases upon compression for silica-poor liquids, but anomalously decreases upon compression for liquids that are silica-rich; similarly, the diffusivity decreases upon compression for silica-poor liquids, but anomalously increases upon compression for silica-rich liquids. For liquids with intermediate silica fraction, similar to basaltic and peridotitic liquids, there is comparatively little change in viscosity or oxygen diffusivity at pressures between 0 and 20 GPa. These results are in good general

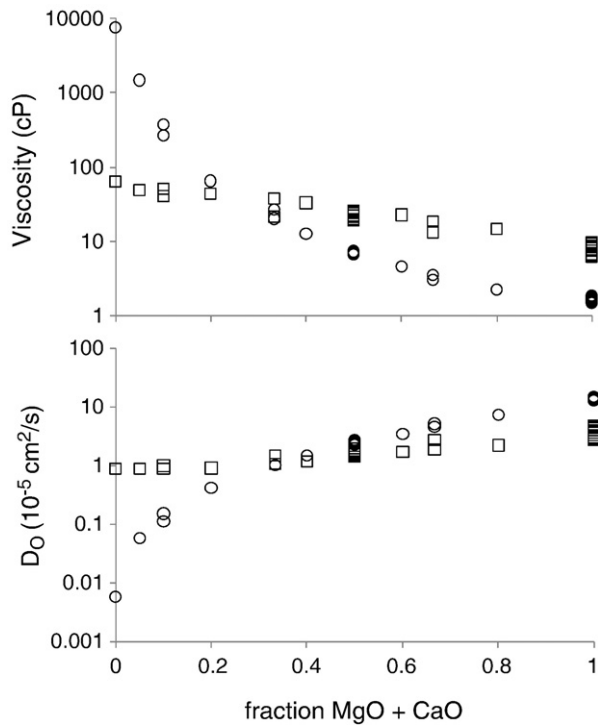


Fig. 4. Viscosity and oxygen diffusivity for all compositions, as function of SiO<sub>2</sub> content. Circles:  $P=0$  GPa; squares:  $P=20$  GPa.

agreement with experimental viscosity and diffusion results for silicate liquids at high pressures. In silica-rich dacite compositions, Si and O diffusivities increase significantly with pressure up to at least 5 GPa (Tinker and Lesher, 2001) and viscosity decreases with pressure over a similar pressure interval (Tinker et al., 2004). In intermediate diopside (Reid et al., 2001; Reid et al., 2003) and peridotite (Liebske et al., 2005) liquids, in contrast, there is comparatively little change in Si and O diffusivities or viscosity at pressures up to  $\sim 15$  GPa.

### 3.3. Transport properties: Effect of Ca/Mg ratio

Fig. 5 shows the results for viscosity, silicon diffusivity and oxygen diffusivity as functions of pressure along the MgSiO<sub>3</sub>–CaSiO<sub>3</sub> join. First we note that for the diffusivities a slight anomalous effect is evident at  $P < 5$  GPa, where the diffusivity increases with increasing pressure; at higher pressure, the normal pressure effect is found, where the diffusivity decreases with increasing pressure. For the viscosity, there is no anomalous viscosity decrease with increasing pressure, but the viscosity essentially remains unchanged between 0 and 5 GPa.

In regard to the effects of the Ca/Mg ratio, Fig. 5 shows a subtle difference in behavior for the viscosity and Si diffusivity in comparison with the O diffusivity. The viscosity and Si diffusivity are independent of the Ca/Mg ratio at low pressure, but vary systematically with the Ca/Mg ratio as the pressure increases; in particular, the viscosity increases, and the Si diffusivity decreases, with increasing Ca/Mg ratio. In contrast, the O diffusivity has essentially the same dependence on the Ca/Mg ratio at all pressures. These contrasting behaviors are more clearly evident in Fig. 6, which shows the change in transport properties as a function of Ca/Mg ratio at 0 GPa and at 20 GPa. Again, the viscosity and Si diffusivity are independent of the Ca/Mg ratio at  $P=0$ , but change with the Ca/Mg ratio at  $P=20$  GPa. In contrast, the O diffusivity changes nearly identically with the Ca/Mg ratio at  $P=0$  and  $P=20$  GPa.

While the influence of Ca/Mg ratio on the transport properties is rather small at 3000 K, we believe that it may be considerably larger in magnitude at lower temperatures.

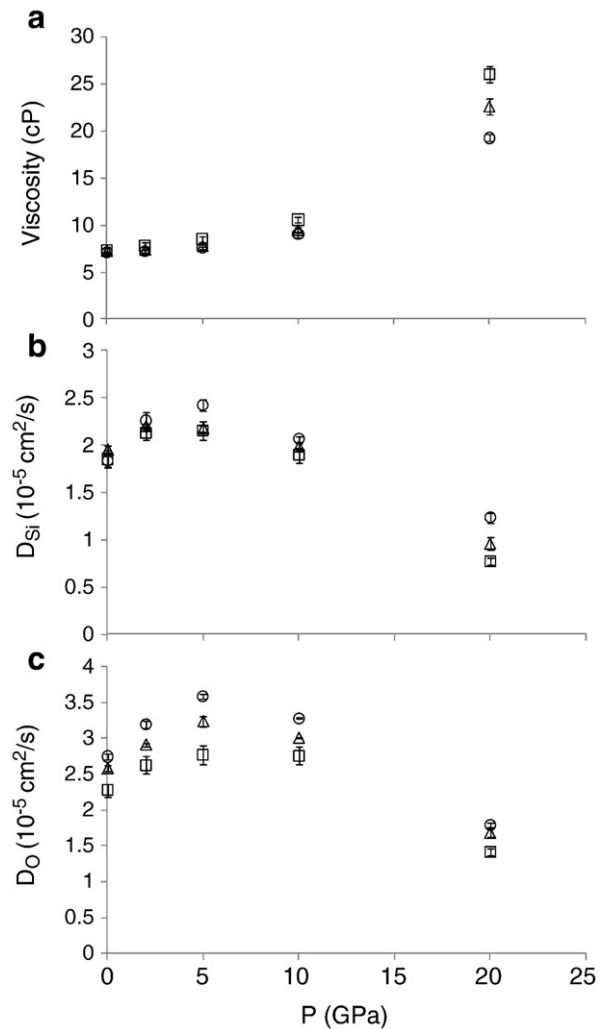
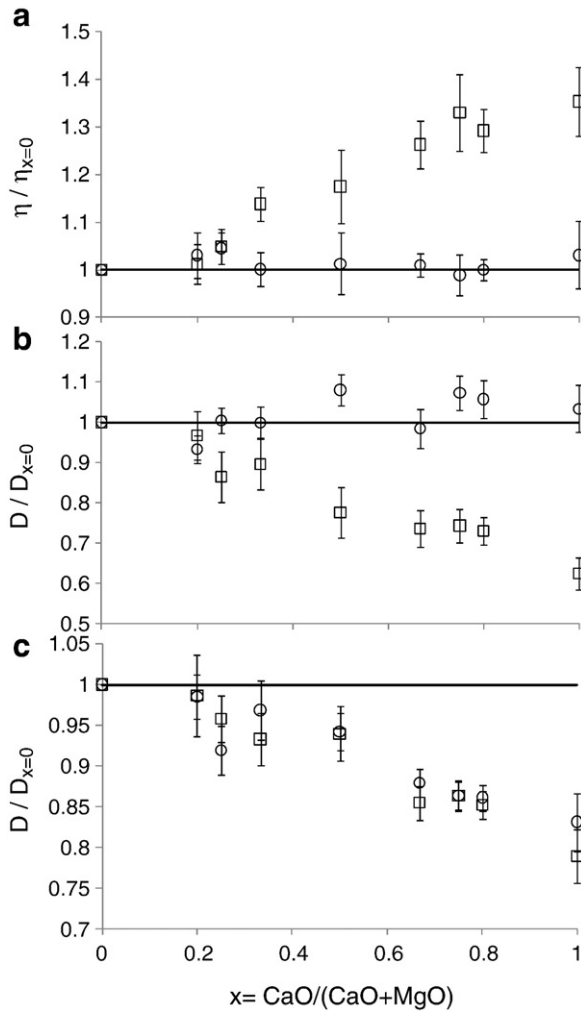


Fig. 5. Results for the CaSiO<sub>3</sub>–MgSiO<sub>3</sub> system showing how transport properties change with pressure. (a) Viscosity; (b) silicon diffusivity; and (c) oxygen diffusivity. Circles: MgSiO<sub>3</sub>; triangles: Ca<sub>1/2</sub>Mg<sub>1/2</sub>SiO<sub>3</sub>; squares: CaSiO<sub>3</sub>.

### 3.4. Apparent activation volumes

Apparent activation volumes for viscosities and ion diffusivities are calculated using the Arrhenius equation (Eq. (5) or (6)). For a given composition, apparent activation volumes at low pressure are based on the change in diffusivity (or viscosity) between  $P=0$  GPa and  $P=2$  GPa, while apparent activation volumes at high pressure are based on changes between  $P=10$  GPa and  $P=20$  GPa. Fig. 7 shows the activation volumes for viscosity and ion diffusivity as a function of the SiO<sub>2</sub> fraction of the liquid. At low pressure, the activation volumes for Si diffusion, O diffusion and viscosity vary systematically from negative values to positive values as the SiO<sub>2</sub> fraction decreases (Fig. 7a). As a negative value of the apparent activation volume indicates anomalous pressure dependence, the presence or absence of the anomalous pressure dependence is seen to be primarily a function of SiO<sub>2</sub> fraction. At higher pressure (10–20 GPa) the apparent activation volumes for Si diffusion, O diffusion and viscosity are small, and positive except in very high silica compositions; across the entire range of composition, there is little variation in the apparent activation volumes.

The dependences of the apparent activation volumes for Ca and Mg diffusivity (Fig. 7b) are quite different than those for O and Si diffusivity or viscosity. There is no significant variation of the apparent activation volumes of Ca and Mg diffusion with the SiO<sub>2</sub> fraction, and their values are similar at low pressure and high pressure.



**Fig. 6.** Results for the  $\text{CaSiO}_3$ – $\text{MgSiO}_3$  system showing how transport properties change with Ca/Mg ratio. (a) Viscosity; (b) Si diffusivity; and (c) O diffusivity. Circles:  $P=0$  GPa; squares:  $P=20$  GPa.

Fig. 8 shows the apparent activation volumes along the  $\text{CaSiO}_3$ – $\text{MgSiO}_3$  join. At low pressure, the values for Si and O diffusivity are significantly negative, the values based on viscosity are close to zero, and the values based on Mg and Ca diffusivity are significantly positive. However, at high pressure, the apparent activation volumes based on all transport properties are very similar (and slightly positive). These results have implications in regard to Eyring-like correlations often used to relate the diffusivity and viscosity (e.g., Shimizu and Kushiro, 1984; Poe et al., 1997; Reid et al., 2001; Mungall, 2002; Tinker et al., 2004): at low pressure, viscosity and diffusivity clearly behave differently, indicating that a correlation between them is not so simple. In contrast, a clear correlation appears to exist at high pressure.

For liquids along the CaO–MgO join, there is a systematic increase in the apparent activation volume for viscosity with increasing CaO content, at both low and high pressures (Fig. 9a). The increase in apparent activation volume follows the increase in the molar volume of the liquid with increasing CaO, such that the ratio of apparent activation volume to molar volume is nearly constant at a given pressure (Fig. 9b). With increasing pressure, the apparent activation volume becomes a smaller proportion of the molar volume: at 0–2 GPa, the apparent activation volume for viscosity is ~25% of the molar volume, while at 10–20 GPa the apparent activation volume is only ~9% of the molar volume. In other words, the apparent activation volume for the viscosity of these liquids is significantly more compressible than the liquids themselves.

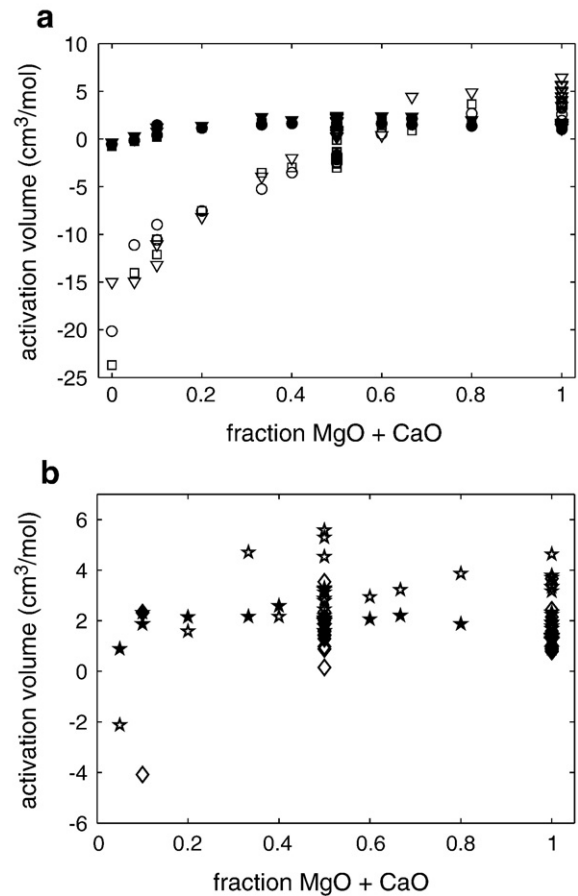


**Fig. 7.** Apparent activation volumes for all compositions, as a function of  $\text{SiO}_2$  content. (a) Activation volumes for Si diffusivity (squares), O diffusivity (circles) and viscosity (triangles); and (b) Activation volumes for Mg (diamonds) and Ca (stars). Open symbols are for low pressure (0–2 GPa), closed symbols for 10–20 GPa.

#### 4. Discussion

Our main results can be understood in terms of the liquid structures of the components. The MgO and CaO liquids have structures in which the atoms are close packed at all pressures. In contrast, the structure of liquid  $\text{SiO}_2$  at low pressure is an open network structure based on linked  $\text{SiO}_4$  tetrahedra. If these linked  $\text{SiO}_4$  tetrahedra percolate through the system ('polymerized'), the atoms are somewhat 'locked in place' by the network, resulting in high viscosity and low diffusivity. The polymerized structure can be broken in two ways: (1) by incorporating other ions (e.g., Mg, Ca) that disrupt the connectivity of  $\text{SiO}_4$  tetrahedra; and (2) by high pressure, which makes the denser, close-packed structure more stable than the less dense, open network structure.

At low pressure, the open network structure of the  $\text{SiO}_2$  component is the critical factor in the system properties, which has the following implications:

- i. *Mixing is highly non-ideal except when the fraction of  $\text{SiO}_2$  is constant.* This effect is demonstrated in Fig. 3a, in that the excess molar volume is generally significant, and is nearly zero only for mixtures where the fraction of  $\text{SiO}_2$  is unchanged (e.g., along the  $\text{MgSiO}_3$ – $\text{CaSiO}_3$  join). The non-ideal mixing stems from the incommensurate nature of the open network structure of  $\text{SiO}_2$  and the close packed structures of MgO and CaO. Since MgO and CaO have similar close packed structures, their mixing is nearly ideal. Similarly, because  $\text{CaSiO}_3$  and  $\text{MgSiO}_3$  liquids have similar structures, which are neither fully

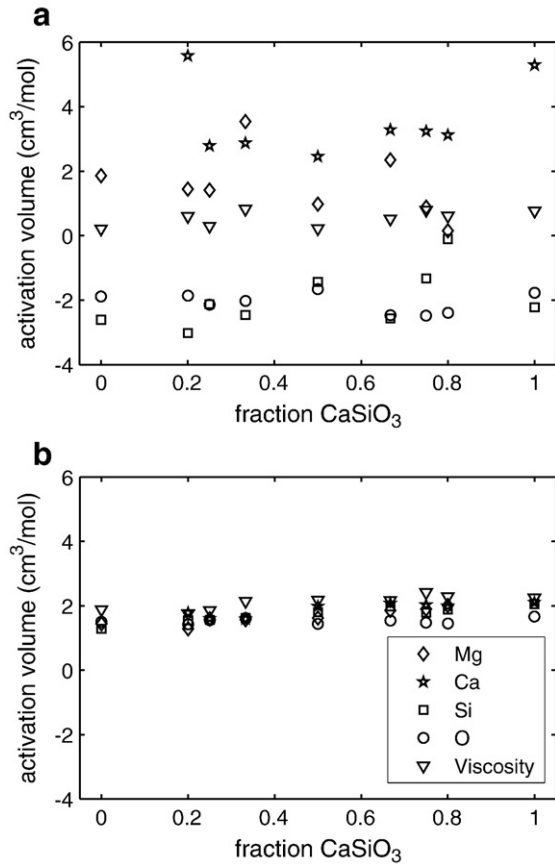


**Fig. 8.** Apparent activation volumes along the CaSiO<sub>3</sub>–MgSiO<sub>3</sub> join. (a) Low pressure (0–2 GPa); and (b) High pressure (10–20 GPa).

polymerized nor close-packed, their mixing is also nearly ideal.

- ii. *SiO<sub>2</sub> fraction is the primary factor that controls the viscosity and diffusivity in these systems, especially at low pressure.* This result is well known (e.g. Mysen, 1988), and it occurs because the SiO<sub>2</sub> fraction determines whether the SiO<sub>4</sub> tetrahedra are polymerized: the linked SiO<sub>4</sub> tetrahedra are polymerized at high SiO<sub>2</sub> fraction, but not at low SiO<sub>2</sub> fraction. Since the polymerized structures lead to high viscosity and low diffusivity, and the extent of polymerization is determined by the SiO<sub>2</sub> fraction, it follows that the viscosity, and the diffusivity of network-forming ions, will depend strongly on SiO<sub>2</sub> fraction.
- iii. *The O diffusivity depends on the Ca/Mg ratio, but the Si diffusivity does not.* Oxygen ions are nearest neighbors of Ca or Mg. As the Ca/Mg ratio changes, the average local environment around the O ions changes and the diffusivity of O does as well. In contrast, Si ions are not nearest neighbors of Ca or Mg, and changes in their ratio do not appreciably influence the local environment around Si or its diffusivity.

At high pressures, the open network of linked SiO<sub>4</sub> tetrahedra is no longer relevant, and instead SiO<sub>2</sub> and all other liquids in the system are close packed. This fundamental change in liquid structure at high pressures has the following implications:

- i. *Mixing is nearly ideal for all systems at high pressure (regardless of changes in SiO<sub>2</sub> fraction).* Fig. 3b shows that the excess volume of mixing is nearly zero for all mixtures at high pressure. This occurs because at high pressure the SiO<sub>2</sub>, MgO and CaO liquids all have close packed structures — because the structures of the liquids are similar, their mixing is nearly ideal.

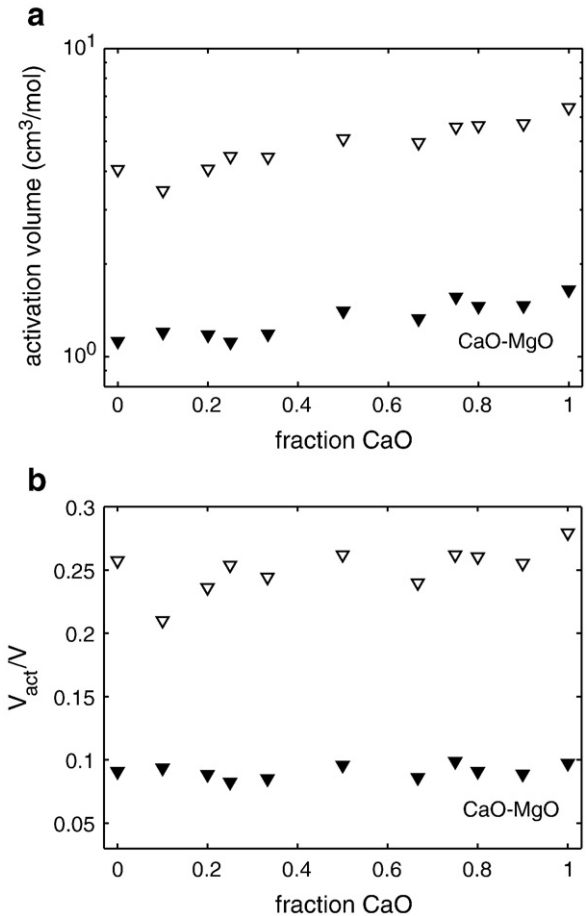


**Fig. 9.** Apparent activation volume for viscosity along the CaO–MgO join. (a) Activation volume; and (b) Activation volume divided by molar volume. Open symbols, 0–2 GPa; Closed symbols 10–20 GPa.

- ii. *The viscosity and Si diffusivity depend significantly on the Ca/Mg ratio at high pressure.* As shown in Fig. 6, the viscosity increases and the Si diffusivity decreases with increasing Ca/Mg ratio. This dependence occurs because the Ca ion is larger than the Mg ion, and the larger size restricts atomic mobility when the ions are pushed closely together, as happens at high pressure (Zhang et al., 2009). Hence, the viscosity increases and Si diffusion is impeded as Mg is replaced by the larger Ca cation. The dependence on Ca/Mg ratio is not significant at low pressure because in this case the liquid can expand to accommodate the larger ion. The low-pressure behavior observed in our simulations is consistent with the experimental database on silicate melt viscosity, which can be modeled successfully by considering only the total content of structure-modifying species without regard to their identities (Giordano and Dingwell, 2003). At higher pressures, our results suggest that the transport properties of a melt will depend more strongly on the radii of the constituent ions.

Regarding the changes in viscosity and diffusivity with pressure, there are two mechanisms to consider for silicate liquids. First, increasing pressure decreases the free volume and thus decreases atomic mobility; acting alone, this mechanism leads to ‘normal’ behavior, where the viscosity increases and the diffusivity decreases with increasing pressure. Second, pressure acts to destroy the network structure of SiO<sub>4</sub> tetrahedra, which as discussed above hinders atomic mobility; in this way, pressure acts to increase atomic mobility, leading to ‘anomalous’ behavior where the viscosity decreases and the diffusivity increases with increasing pressure. The apparent activation

volume is positive for 'normal' changes in transport properties (described above), and it is negative for anomalous changes. Implications of these structural considerations are as follows:

- i. *At low pressure, apparent activation volumes of viscosity, and Si and O diffusivities, are primarily functions of SiO<sub>2</sub> fraction.* The 'normal' and 'anomalous' mechanisms for changes in viscosity and diffusivity, as described above, act in opposite directions. The normal mechanism applies for all systems, but the anomalous mechanism only applies to polymerized structures. For silica-rich compositions, the structures are polymerized, and the anomalous mechanism dominates the normal mechanism at low pressures. For silica-poor compositions, the structures are not polymerized, and the normal mechanism dominates. Thus, as shown in Fig. 7, the apparent activation volumes range from strongly negative values for silica-rich compositions to positive values for silica-poor compositions. This trend is in broad agreement with experimental data on the viscosity of silicate liquids (Scarfe et al., 1987).
- ii. *At low pressure, apparent activation volumes for Ca and Mg diffusivities have a much weaker dependence on the SiO<sub>2</sub> fraction than the Si and O diffusivities.* As shown in Fig. 7, the apparent activation volumes vary with composition over a much smaller range for Ca and Mg diffusivities than for Si and O diffusivities. This behavior occurs because Ca and Mg are not silicate network formers, and their diffusion is only weakly influenced by changes in the silicate network structure.
- iii. *At high pressure, apparent activation volumes depend nearly as strongly on the Ca/Mg ratio as on the SiO<sub>2</sub> fraction.* This result, which is evident in Fig. 7, occurs because all components have close packed structures at high pressure, and thus play roughly equivalent roles in determining system properties.
- iv. *For CaO–MgO mixtures at a given pressure, the apparent activation volume is a constant fraction of the molar volume of the liquid, regardless of the composition.* This result is evident in Fig. 9b. As pressure increases, the activation volume becomes a smaller fraction of the molar volume. The reduction in activation volume with increasing pressure in these simple oxide liquids may also apply more generally to silicate liquids at very high pressures where all components of the liquid (even SiO<sub>2</sub>) have close-packed structures.

## 5. Conclusions

The main idea from this work is that while the SiO<sub>2</sub> fraction plays a dominant role in determining silicate properties at low pressure – causing dramatic dependences of viscosity and diffusivity on composition, anomalous pressure dependences of properties, and non-ideal mixing – the SiO<sub>2</sub> fraction does not play a dominant role at high pressure. At high pressure, the properties of silicate liquids are much simpler, in that the viscosity and diffusivity change relatively little with composition, the pressure dependences of transport properties are normal, and mixing is nearly ideal. Similar behavior is also observed in the relationship between viscosity and diffusivity, which follows a simple Eyring-type relation at high pressure but is more complicated at lower pressures. This simplicity arises from the fact that the liquid structures of all components are similar at high pressure, whereas there is a striking difference between the polymerized structure of liquid SiO<sub>2</sub> and the close-packed structures of CaO and MgO at low pressure.

The relatively simple behavior of silicate liquids at high pressure is important for modeling the dynamics of deep magma oceans, and for estimating the properties of melts that may exist in Earth's core-mantle boundary region (Lay et al., 2004). If mixing between melt components is ideal at high pressures, then the density of a melt can be determined based on knowledge of the equations of state of the

end-member components, without the need to consider excess mixing terms (which are difficult to constrain in multicomponent liquids at very high pressures). Similarly, estimating the viscosity and chemical diffusivities of melts at high pressures and temperatures is much simpler if these properties are insensitive to the composition of the melt. The transport properties of simple melts like Mg<sub>2</sub>SiO<sub>4</sub> (de Koker et al., 2008) or MgSiO<sub>3</sub> (Nevins et al., 2009) at high pressures are likely to be similar to those of the multicomponent liquids that are relevant to deep planetary interiors.

## Acknowledgments

We thank the National Science Foundation (grant EAR-0635820) for support of this research, the Ohio Supercomputer Center for computational resources, and two anonymous reviewers for constructive comments that helped improve the manuscript.

## References

- Adjaoud, O., Steinle-Neumann, G., Jahn, S., 2008. Mg<sub>2</sub>SiO<sub>4</sub> liquid under high pressure from molecular dynamics. *Chem. Geol.* 256, 185–192.
- Alfè, D., 2005. Melting curve of MgO from first-principles simulations. *Phys. Rev. Lett.* 94, Art. No. 235701.
- Behrens, H., Schulze, F., 2003. Pressure dependence of melt viscosity in the system NaAlSi<sub>3</sub>O<sub>8</sub>–CaMgSi<sub>2</sub>O<sub>6</sub>. *Am. Mineral.* 88, 1351–1363.
- Ben Martin, G., Spera, F.J., Ghiorso, M.S., Nevins, D., 2009. Structure, thermodynamic, and transport properties of molten Mg<sub>2</sub>SiO<sub>4</sub>: molecular dynamics simulations and model EOS. *Am. Mineral.* 94, 693–703.
- Bryce, J.G., Spera, F.J., Stein, D.J., 1999. Pressure dependence of self-diffusion in the NaAlO<sub>2</sub>–SiO<sub>2</sub> system: Compositional effects and mechanisms. *Am. Mineral.* 84, 345–356.
- de Koker, N.P., Stixrude, L., Karki, B.B., 2008. Thermodynamics, structure, dynamics and freezing of Mg<sub>2</sub>SiO<sub>4</sub> liquid at high pressure. *Geochim. Cosmochim. Acta* 72, 1427–1441.
- Giordano, D., Dingwell, D.B., 2003. Non-Arrhenian multicomponent melt viscosity: a model. *Earth Planet. Sci. Lett.* 208, 337–349.
- Karki, B.B., Bhattarai, D., Stixrude, L., 2006. First-principles calculations of the structural, dynamical, and electronic properties of liquid MgO. *Phys. Rev. B* 73, Art No. 174208.
- Karki, B.B., Bhattarai, D., Stixrude, L., 2007. First-principles simulations of liquid silica: structural and dynamical behavior at high pressure. *Phys. Rev. B* 76, Art No. 104205.
- Kubicki, J.D., Muncill, G.E., Lasaga, A.C., 1990. Chemical diffusion in melts on the CaMgSi<sub>2</sub>O<sub>6</sub>–CaAl<sub>2</sub>Si<sub>2</sub>O<sub>8</sub> join under high pressures. *Geochim. Cosmochim. Acta* 54, 2709–2715.
- Lacks, D.J., Van Orman, J.A., 2007. Molecular dynamics investigation of viscosity, chemical diffusivities and partial molar volumes of liquids along the MgO–SiO<sub>2</sub> join as functions of pressure. *Geochim. Cosmochim. Acta* 71, 1312–1323.
- Lay, T., Garnero, E.J., Williams, Q., 2004. Partial melting in a thermo-chemical boundary layer at the base of the mantle. *Phys. Earth Planet. Inter.* 146, 441–467.
- Leshner, C.E., Hervig, R.L., Tinker, D., 1996. Self diffusion of network formers (silicon and oxygen) in naturally occurring basaltic liquid. *Geochim. Cosmochim. Acta* 60, 405–413.
- Liebske, C., Schmickler, B., Terasaki, H., Poe, B.T., Suzuki, A., Funakoshi, K.-I., Ando, R., Rubie, D.C., 2005. Viscosity of peridotite liquid up to 13 GPa: implications for magma ocean viscosities. *Earth Planet. Sci. Lett.* 240, 589–604.
- Mikkelsen Jr., J.C., 1984. Self diffusivity of network oxygen in vitreous SiO<sub>2</sub>. *Appl. Phys. Lett.* 45, 1187–1189.
- Mungall, J.E., 2002. Empirical models relating viscosity and tracer diffusion in magmatic silicate melts. *Geochim. Cosmochim. Acta* 66, 125–143.
- Mysen, B.O., 1988. Structure and Properties of Silicate Melts. Elsevier, Amsterdam. 354 pp.
- Nevins, D., Spera, F.J., Ghiorso, M.S., 2009. Shear viscosity and diffusion in Liquid MgSiO<sub>3</sub>: Transport properties and implications for terrestrial planet magma oceans. *Am. Mineral.* 94, 975–980.
- Plimpton, S., 1995. Fast parallel algorithms for short-range molecular dynamics. *J. Comput. Phys.* 117, 1–19.
- Plimpton, S., Pollock, R., Stevens, M., 1997. Particle-mesh Ewald and rRESPA for parallel molecular dynamics simulations. In: Heath, M., Torczon, V., Astfalk, G., Bjorstad, P.E., Karp, A.H., Koebel, C.H., Kumar, V., Lucas, R.F., Watson, L.T., Womble, D.E. (Eds.), Proceedings of the Eighth SIAM Conference on Parallel Processing for Scientific Computing. SIAM, Philadelphia. CD-ROM, ISBN 0-89871-395-1.
- Poe, B.T., McMillan, P.F., Rubie, D.C., Chakraborty, S., Yarger, J., Diefenbacher, J., 1997. Silicon and oxygen self diffusivities in silicate liquids measured to 15 gigapascals and 2800 kelvin. *Science* 276, 1245–1248.
- Reid, J.E., Poe, B.T., Rubie, D.C., Zotov, N., Wiedenbeck, M., 2001. The self-diffusion of silicon and oxygen in diopside (CaMgSi<sub>2</sub>O<sub>6</sub>) liquid up to 15 GPa. *Chem. Geol.* 174, 77–86.
- Reid, J.E., Suzuki, A., Funakoshi, K.I., Terasaki, H., Poe, B.T., Rubie, D.C., Ohtani, E., 2003. The viscosity of CaMgSi<sub>2</sub>O<sub>6</sub> liquid at pressures up to 13 GPa. *Phys. Earth Planet. Inter.* 139, 45–54.
- Scarfe, C.M., Mysen, B.O., Virgo, D., 1987. Pressure dependence of the viscosity of silicate melts. In: Mysen, B.O. (Ed.), *Magmatic Processes: Physicochemical Principles*, Special Publication: The Geochemical Society, vol. 1, pp. 504–511.
- Shimizu, N., Kushiro, I., 1984. Diffusivity of oxygen in jadeite and diopside melts at high pressures. *Geochim. Cosmochim. Acta* 48, 1295–1303.

- Speziale, S., Zha, C.-S., Duffy, T.S., Hemley, R.J., Mao, H.-K., 2001. Quasi-hydrostatic compression of magnesium oxide to 52 GPa: implications for the pressure-volume-temperature equation of state. *J. Geophys. Res.* 106, 515–528.
- Speziale, S., Shieh, S.R., Duffy, T.S., 2006. High-pressure elasticity of calcium oxide: a comparison between Brillouin spectroscopy and radial X-ray diffraction. *J. Geophys. Res.* 111, Art. No. B02203.
- Stixrude, L., Karki, B., 2005. Structure and freezing of MgSiO<sub>3</sub> liquid in Earth's lower mantle. *Science* 310, 297–299.
- Suzuki, A., Ohtani, E., Funakoshi, K., Terasaki, H., Kubo, T., 2002. Viscosity of albite melt at high pressure and high temperature. *Phys. Chem. Miner.* 29, 159–165.
- Tinker, D., Leshner, C.E., 2001. Self diffusion of Si and O in dacitic liquid at high pressures. *Am. Mineral.* 86, 1–13.
- Tinker, D., Leshner, C.E., Hutcheon, I.D., 2003. Self-diffusion of Si and O in diopside–anorthite melt at high pressures. *Geochim. Cosmochim. Acta* 67, 133–142.
- Tinker, D., Leshner, C.E., Baxter, G.M., Uchida, T., Wang, Y., 2004. High-pressure viscometry of polymerized silicate melts and limitations of the Eyring equation. *Am. Mineral.* 89, 1701–1708.
- van Beest, B.W.H., Kramer, G.J., van Santen, R.A., 1990. Force fields for silicas and aluminophosphates based on ab initio calculations. *Phys. Rev. Lett.* 64, 1955–1958.
- Zhang, L., Van Orman, J.A., Lacks, D.J., 2009. The influence of atomic size and charge of dissolved species on the diffusivity and viscosity of silicate melts. *Am. Mineral.* 94, 1735–1738.